ELSEVIER

Marine Geology 149 (1998) 211–228

MARINE GEOLOGY
INTERNATIONAL JOURNAL OF MARINE GEOLOGY, GEOCHEMISTRY AND GEOPHYSICS

Late Quaternary iceberg-rafted detritus events on the Denmark Strait–Southeast Greenland continental slope (∼65ºN): related to North Atlantic Heinrich events?

J.T. Andrews [a,*], T.A. Cooper [a], A.E. Jennings [a], A.B. Stein [a], H. Erlenkeuser [b]

[a] *Institute of Arctic and Alpine Research and Department of Geological Sciences, University of Colorado, Box 450, Boulder, CO 80309, USA*

[b] *Leibniz-Laboratory for Radiometric Dating and Stable Isotope Research, Kiel University, Max-Eyth-Straße 11, D-24118 Kiel, Germany*

Received 15 October 1997; accepted 27 February 1998

Abstract

HU93030-007 LCF (65º01.39′N and 30º14.81′W) is a 4.5 m long, giant (11 cm diameter) piston core from 1800 m water depth on the continental slope, south of the Denmark Strait sill. The core sampled acoustically stratified sediments at a site below the Kangerlussuaq Trough. Nine AMS ^{14}C dates on planktic foraminifera indicate that the core spans ∼14 to 28 ^{14}C ka. The sediments consists of two principal lithofacies: Lithofacies I (LI) comprises tan/ochre intervals with abundant ice-rafted sandstone/siltstone clasts larger than 2 mm and with an average thickness of 47 cm; it is also associated with peaks in carbonate content and TOC%. Lithofacies II (LII) consists of fine-grained, dark gray, hemipelagic sediment. There are three distinct intervals of LI dated between 14.3 and 15.5 (LIc), 20.1 and 21.9 (LIb), 24.7 and 25.8 (LIa) ka. The ages suggest that deposition of LI is approximately coeval with Heinrich events 1 and 2 in the North Atlantic, whereas LIa appears younger than H-3. Lithofacies I is derived from far-travelled ice bergs from an unknown source, but not from the northeastern Laurentide Ice Sheet. Stable isotope studies on *Neogloboquadrina pachyderma* sinistral show little evidence for significant meltwater events associated with LI, but surprisingly, light oxygen isotopic events are present in the benthic foraminiferal analyses (*Cibicidoides wuellerstorfi* and *Melonis zaandamae*). The ages of the HU93030-007 iceberg-rafted detritus (IRD) events are similar to IRD peaks in cores north of Denmark Strait, on the East Greenland slope. HU87033-009 LCF (SE Baffin slope, 62º30.99′N and 59º26.82′W, 1437 m wd) is situated in a similar position to HU93030-007 but with respect to the Laurentide Ice Sheet; its $\delta^{18}O$ record on planktic foraminifera is virtually identical to that of HU93030-007. The timing of IRD events is similar in both these cores between 14 and 30 ka. H-3 may be present in HU87033-009 as an IRD event, but in contrast to H-1 and H-2, it is not evident as a discernible detrital carbonate event.

Keywords: Heinrich events; iceberg rafting; Denmark Strait; late Quaternary

* Corresponding author. Tel.: +1 (303) 492-5183; Fax: +1 (303) 492-6388; E-mail: andrewsj@spot.colorado.edu

0025-3227/98/$19.00
PII S0025-3227(98)00029-2

1. Introduction

Many studies have used the numerous sediment cores collected throughout the North Atlantic and Nordic Seas regions to reconstruct paleoceanographic histories (Keigwin and Boyle, 1989; Koc and Jansen, 1994; Sarnthein et al., 1995). Recently, studies have focused on identifying discrete iceberg-rafted detritus (IRD) strata, now commonly referred to as Heinrich (H-) events (Heinrich, 1988; Bond et al., 1992; Broecker et al., 1992; Grousset et al., 1993; Bond and Lotti, 1995; Dowdeswell et al., 1995; Robinson et al., 1995). These layers are postulated to be the result of the melting of massive armadas of icebergs being discharged from Northern Hemisphere Ice Sheets, more specifically the Laurentide Ice Sheet (Alley and MacAyeal, 1994).

Along with this discovery has been a growing debate as to the source of the material that makes up the Heinrich layers and ultimately the mechanism(s) which contributes the distinctive sediments of the H-events. The two sides of the debate can be summarized as follows: (1) Heinrich events consist mainly of material delivered by periodic surges of the Laurentide Ice Sheet that are the result of internal glaciological factors (MacAyeal, 1993; Alley and MacAyeal, 1994; Marshall and Clarke, 1998); or (2) Heinrich layers contain material delivered from the Fennoscandinavian (Rahman, 1995) and Greenland/Iceland ice sheets as well as from the Laurentide Ice Sheet, and they may be the result of climatic forcing (Bond and Lotti, 1995; Fronval et al., 1995). A third scenario might be that the ice sheet reactions are linked in a 'cascade' so that the collapse of one triggers responses in the others, possibly associated with changes in relative sea level adjacent to ice sheet margins. Such changes could significantly affect the calving rate and hence the stability of marine-based ice sheets (Thomas, 1977; Thomas and Bentley, 1978).

Our paper presents new information about iceberg rafting events and glacial history on the East Greenland continental margin west of Denmark Strait. Core HU93030-007LCF, henceforth 007, was taken as part of a project aimed at understanding land/ocean sediment transfers across glaciated continental margins (Andrews, 1990; Syvitski, 1991). We present the chronology, lithofacies, and stable isotopic data from this giant piston core, which was collected from *CSS Hudson* on the slope of East Greenland in 1800 m water depth, with the goal of determining the sedimentary processes and provenance of the sediments (Fig. 1A, Fig. 2). We compare data from this site with evidence from cores upstream along the East Greenland margin (Nam et al., 1995; Stein et al., 1996), and from a comparable site HU8733-009LCF, henceforth 009, adjacent to the Laurentide Ice Sheet in the NW Labrador Sea (Jennings et al., 1996) (Fig. 1A).

2. Background

Denmark Strait is an important and sensitive area for paleoceanographic and paleoclimatic studies (Sarnthein et al., 1995; Sarnthein and Altenbach, 1995) (Fig. 1). Bond (1994) identified the Denmark Strait region as a 'benchmark site' for the study of abrupt climate change in the North Atlantic. It constitutes the western part of the Greenland–Scotland ridge, the 600 m deep physical barrier between the North Atlantic and Nordic seas. Two major ocean currents flow along the continental margin, the East Greenland Current (EGC) and the Irminger Current (IC) (Johannessen, 1986; Swift, 1986; Aagard et al., 1991) (Fig. 1A). The EGC flows southward carrying cold, low-salinity Polar Water along the west side of the strait. The IC flows northward bringing warmer, salty Atlantic Water along the east side of the strait before turning and flowing south along the outer East Greenland slope. The boundary between the two currents forms the oceanic Polar Front (Malmberg, 1985). Core 007 (65º01.39′N and 30º14.81′W) is located on the continental slope near the boundary between the EGC and the IC and in the path of the Denmark Strait deep-water overflow. Because of its role in forming North Atlantic Deep Water (NADW), the Denmark Strait Overflow Water (DSOW) has a major influence on the global thermohaline circulation and climate (Swift, 1986; Broecker and Denton, 1989). Deep-water boundary currents sweep along the continental slopes south of Denmark Strait, directed along general east to west trajectories (McCave and Tucholke, 1986).

Published core data in Denmark Strait are limited and focus predominantly on one core V28-14

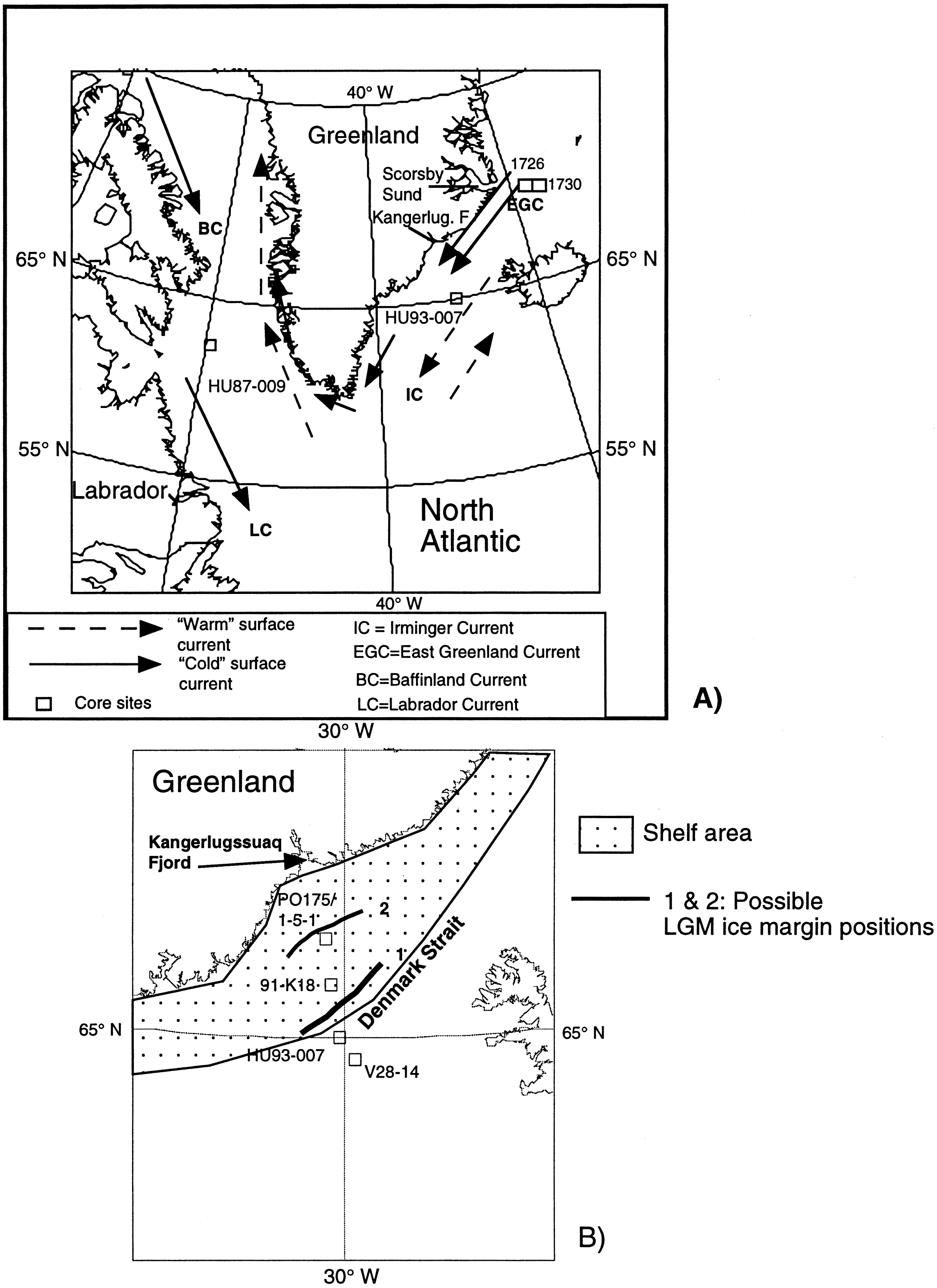

Fig. 1. (A) Map of the North Atlantic showing the location of cores HU93030-007, HU87033-009, PS1726 and PS1730, and present-day surface currents. (B) Location map showing the area of Denmark Strait and the location of HU93030-007, V28-14, and other cores noted in the text. Lines marked *1* and *2* represent possible margins of the East Greenland Ice Sheet during the LGM (1, Stein, 1996; 2, Andrews et al., 1996). The shelf break corresponds to a water depth of around 300 m.

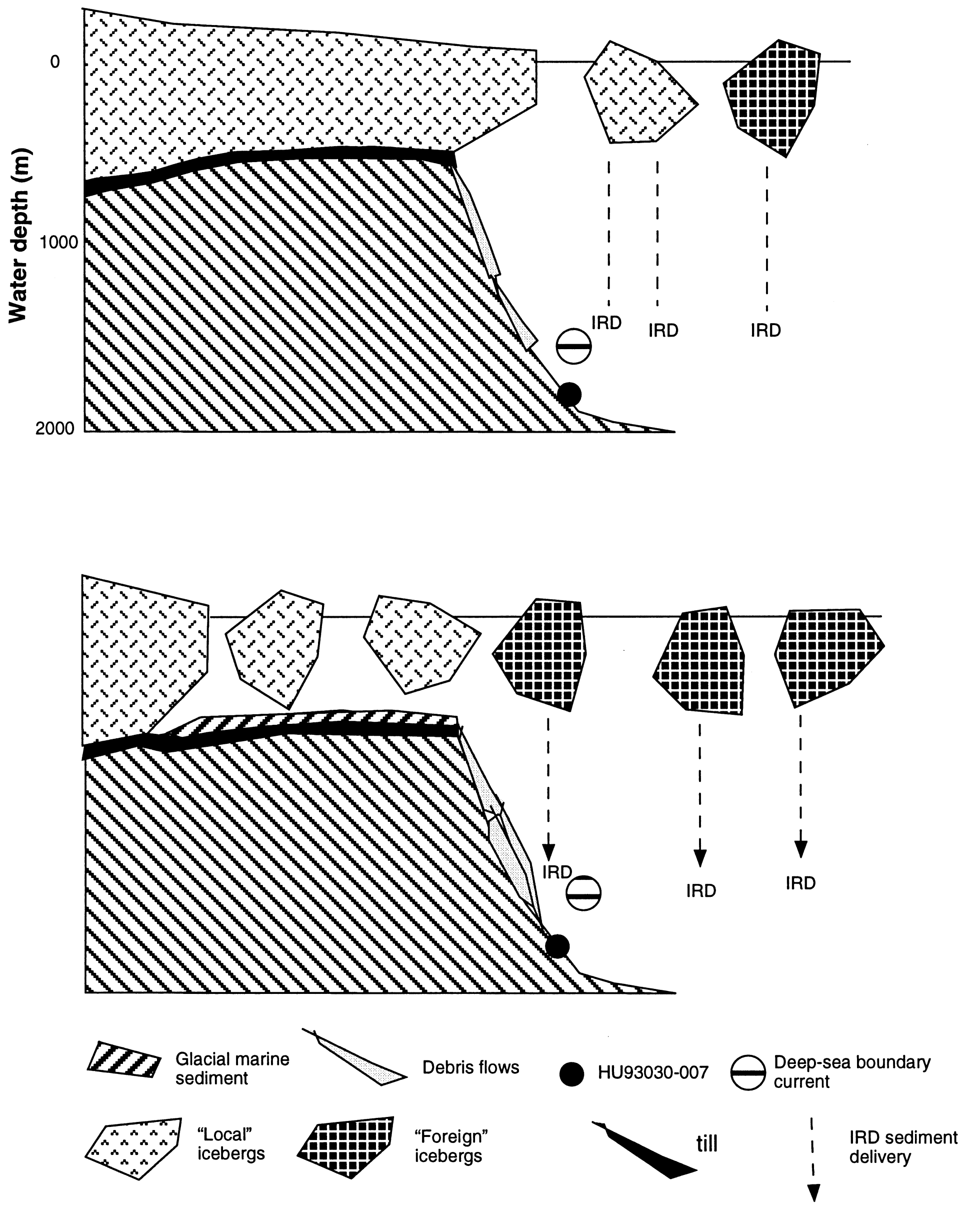

Fig. 2. Scenarios for deposition of the clast-rich intervals in HU93030-007 (i.e. see Fig. 5).

(64º47′N, 29º34′W; 1855 m wd) (Kellogg, 1984; Bond and Lotti, 1995) (Fig. 1B), several new studies have recently been submitted for publication (e.g. Voelker et al., 1997; Lackschewitz et al., 1998). These paleoceanographic studies have lacked information about the glacial extent and history from the bordering continental shelves of Iceland and East Greenland (cf. Denton and Hughes, 1981, see minimum and maximum reconstructions). The location of the margin of the Greenland Ice Sheet at the last glacial maximum (LGM) is uncertain and speculative (Funder, 1989; Andrews et al., 1996; Funder and Hansen, 1996; Stein, 1996). Fig. 1B shows two recent suggestions (e.g. 1, Stein, 1996; 2 Andrews et al., 1996).

Immediately south of Denmark Strait, the East

Greenland continental shelf reaches its greatest width of 300 km. This part of the shelf is cut by Kangerlussuaq Trough which trends roughly N–S toward Kangerlussuaq Fjord (Sommerhoff et al., 1979; Sommerhoff, 1981; Mienert et al., 1992). The late Quaternary sedimentation and chronology along Kangerlussuaq Trough have been described by Mienert et al. (1992), Williams (1993), Williams et al. (1995) and Andrews et al. (1996). Stein (1996) undertook a detailed study of the continental margin evolution using seismic data along the trough and onto the adjacent slope. Nam et al. (1995) and Stein et al. (1996) have presented data on iceberg rafting and paleoceanography along shelf/slope transects off Scoresby Sund (Fig. 1A).

Core 007 was taken to establish a record of glacial activity on the East Greenland continental shelf/slope, and ice sheet/ocean interactions in the Denmark Strait.

Table 1
Radiocarbon dates on HU93030-007LCF and TWC — all on *N. pachyderma* sinistral

Depth (cm)	Lab. No. (uncorrected)	Age (year)	Comments
7	AA-13238	$15,270 \pm 120$	in Lithofacies Ic
45	AA-17389	$15,760 \pm 140$	immediately below Ic
90	AA-15704	$17,165 \pm 140$	in IIc
150	AA-13239	$19,635 \pm 150$	in IIc
215	AA-15705	$22,110 \pm 230$	in Ib
284	AA-15706	$22,225 \pm 245$	in IIb
341	AA-14215	$25,330 \pm 310$	in Ia
375	AA-15707	$27,130 \pm 335$	at boundary IIa/Ia
445	AA-12898	$28,005 \pm 350$	in IIa
Lithofacies	**Boundary**	**Age**	
Ic	0 cm	14.31 ± 0.05	
Ic	40 cm	15.51 ± 0.06	
Ib	190 cm	20.11 ± 0.08	
Ib	250 cm	21.95 ± 0.1	
Ia	340 cm	24.7 ± 0.14	
Ia	380 cm	25.89 ± 0.18	
Depth (cm)	**Age**	**Comments**	
Data from HU87030-009 (Fig. 1A)			
501	14.53 ± 0.1	base of H-1	
651	20.33 ± 0.68	top of H-2	
711	20.62 ± 0.22	base of H-1	
974	33.56 ± 0.68	above H-4	

AA, University of Arizona AMS facility.
Regression equation (450 year ocean correction): age (ka) $= 14.29$ $(\pm 0.25) + 0.0307$ $(\pm 0.00125) \times$ depth (cm), $n = 9$, $r^2 = 0.97$.
Rate of sediment accumulation (SAR) ~31 cm/ka.
North Atlantic: H-1, 14.5 ± ka; H-2: 20.5 ± ; H-3: 27 ±.
Rate of sediment accumulation (SAR) ~39 cm/ka.

3. Materials and methods

Core 007 is a 4.5 m long, 11 cm diameter core. Upon retrieval, whole-core magnetic susceptibility (MS) was measured at 5 cm intervals using a Bartington Magnetic Susceptibility Meter model MS2 with a 12.5 cm diameter loop. In addition to whole-core MS, discrete mass-specific MS and rock magnetic properties (Thompson and Oldfield, 1986; King and Channell, 1991) were later measured. After longitudinal splitting, the working half was subsampled for bulk density, water content, salinity, paleomagnetism, foraminifera, diatoms, stable isotopes, sedimentology, and radiocarbon dating (Table 1). The archive half was visually logged (F.J. Hein, in Asprey et al., 1994, HU93030 Cruise report), photographed, and the sediment color was measured using the 'Colormet'® system. Color was recorded according to the CIE system L, a^*, b^* (cf. Andrews and Freeman, 1996). After the core was transported to the Bedford Institute of Oceanography (Canada), more foraminiferal and stable isotope subsamples were collected to reduce the sample interval to ~10 cm. X-radiography was performed on the archive half. Nine AMS radiocarbon dates on monospecific samples of *N. pachyderma* sinistral were measured at the University of Arizona's Accelerator Mass Spectrometer (AMS) facility both within and between the major IRD intervals (Table 1).

Silt and clay percentages were determined using the Sedigraph 5000D Particle Size Analyzer. Visual counts of the material greater than 2 mm were made from the X-radiographs of the archive-half of the core (Grobe, 1987; Andrews et al., 1997) by counting the number of clasts larger than 2 mm within a 2 by 11 cm window every 2 cm downcore. Thus the measurement, referred to here as ice-rafted detritus (IRD) >2 mm, applies to the number of visible clasts >2 mm/22 cm^2. Total carbonate and the percentages of calcite and dolomite were determined by use of the Chittick apparatus (Dreimanis, 1962).

Total organic carbon (TOC) was determined by the Walkley–Black method (Walkley, 1947).

Subsamples for micropaleontological analysis were weighed wet. The volume of the samples was measured by displacement. The equivalent dry weight of the samples was calculated using the bulk density data. The sediment was washed on a 63 μm sieve to remove the silt and clay fractions, air dried, and dry sieved on a 125 μm sieve. Foraminiferal abundances were calculated by splitting the >125 μm fractions with a soil-test microsplitter to a point at which the known fraction of the subsample thinly covered a standard picking tray. One hundred foraminifera were counted from a random sequence of squares and the total number of foraminifera in each sample was calculated. Foraminiferal concentrations per volume of wet sediment and per gram dry sediment were calculated. Planktonic foraminiferal assemblages were calculated by identifying the 100 individuals picked and calculating percentage data.

We undertook a qualitative survey of the sediment composition, based on six samples, from within and between Lithofacies I (LI) to see if there were any obvious assemblage changes that would provide insight into the origin of the diamictons. We counted ≥300 elements >250 μm and distinguished foraminifera (planktic and benthic), siltstones, poorly lithified sandstones, basalts, quartz, and 'other' rock types. Specifically, we were checking whether there were abundant shelf-dwelling benthic foraminifera within or between the LI units, and what was the distribution of the siltstones.

Stable isotope analyses were made on the subsamples prepared for foraminiferal analysis. Monospecific samples were picked from the >125 μm fraction. *Neogloboquadrina pachyderma* sinistral and *Cibicidoides wuellerstorfi* and/or *Melonis zaandamae* were analyzed for the planktonic and benthic realms, respectively. Samples were run at the University of Kiel, Germany, on an automated CARBO-KIEL CO_2 preparation device which is directly linked to a MAT 251 mass spectrometer. The results are reported relative to PDB (Peedee Belemnite). Replicate samples ($n = 8$) gave differences of 0.03 ± 0.14 on *N. pachyderma* sinistral. *C. wuellerstorfi* was not found at all levels, so to construct a more complete record *M. zaandamae* was also analyzed. Only at four levels were samples of both species available; the average difference was determined to be 0.17‰ (Cooper, 1995, p. 42). The $\delta^{18}O$ values of *M. zaandamae* were thus corrected to *C. wuellerstorfi* values which are offset from inorganic equilibrium $\delta^{18}O$ values by 0.64‰ (Shackleton, 1973).

4. Site details: local seismic stratigraphy and bottom conditions

Bottom photographs at the core site indicate that the sea floor is covered with a current-winnowed layer of gravel, and carbonate (molluscs, echinoderms) hash. The trigger weight corer recovered no sediment. The giant piston corer probably did not 'blow away' much of the coarse bottom sediment. Deep-towed, high-resolution Huntec seismic records indicate that 007 is located in an area of parallel sub-bottom reflections and 007 is confined to seismostratigraphic unit J.3 (Stein, 1996) (Fig. 3). The core intersects two of the major reflections in the upper part of the profile which correlate with lithofacies changes discussed in the next section. Upslope and downslope from 007 there are characteristic surface and subsurface acoustic forms indicative of debris flows (Stein, 1996). The seismic survey coverage is not sufficient to indicate whether the parallel reflections illustrated in Fig. 3 are contourites. However, the seismic architecture is such that we believe that they reflect deposition by deep-water currents that sweep around the North Atlantic (McCave et al., 1995).

5. Results

5.1. Age model

All dates (Cooper, 1995; Manley and Jennings, 1996) were obtained from hand-picked samples of *Neogloboquadrina pachyderma* sinistral (Table 1). For this study, an ocean reservoir correction of 450 years was used, although this correction is unlikely to apply for all periods (Bard et al., 1994). Moreover, variable regional development of the reservoir effect with significantly different amplitudes may apply to

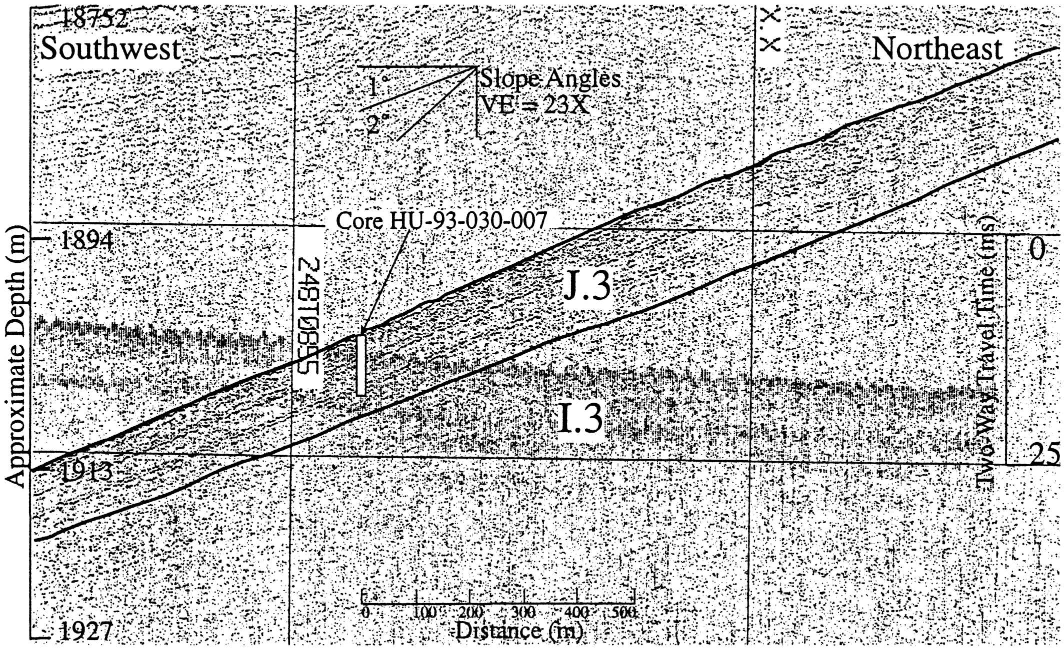

Fig. 3. High-resolution stratigraphy (Huntec DTS) across the coring site for HU93030-007. Seismo-stratigraphic units J.3 and I.3 are identified (Stein, 1996).

Denmark Strait waters in the past (Voelker et al., 1997).

Dates were plotted against depth in the core and a linear equation was fitted to the dates to generate an age model (Fig. 4); higher-order polynomials did not produce statistically significant higher r^2 values. The errors on both the intercept and slope associated with the regression are shown in Table 1. Using robust error estimation (Stata, 1996), the 95% range on the extrapolated age of the core top varies between 13.6 and 14.8 ka indicating virtually no sediment deposition during the Holocene along this section of the East Greenland slope. The ages and errors associated with estimating the ages of the lithofacies boundaries (e.g. Bennett, 1994) were estimated using a Monte Carlo simulation. Thus we generated ten age/depth models, and linear regression equations were calculated for each. These equations were then used to calculate the estimated ages ranges for the lithological boundaries after a 450 year ocean reservoir correction (Table 1).

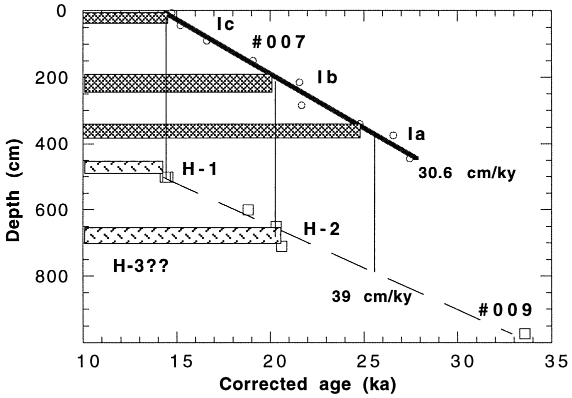

Fig. 4. Depth/age relationship and IRD/Heinrich events for HU93030-007 and HU87033-009 (see Fig. 1A for sites). HU87033-009 is terminated at ~5 m, i.e. during H-2, to allow comparison with HU93030-007. Sediment accumulation rates noted for both cores.

The average sediment accumulation rate (SAR) is 30.6 cm/ka, or ~33 yr/cm. The depth/age relation (Fig. 4; Table 1) indicates the following sampling resolutions: (a) IRD from X-radiography, 60 years; (b) whole-core magnetic susceptibility, 150 years; and (c) isotope and grain-size properties, ~300 years. These differences influenced how we graphed the data (e.g. Fig. 5).

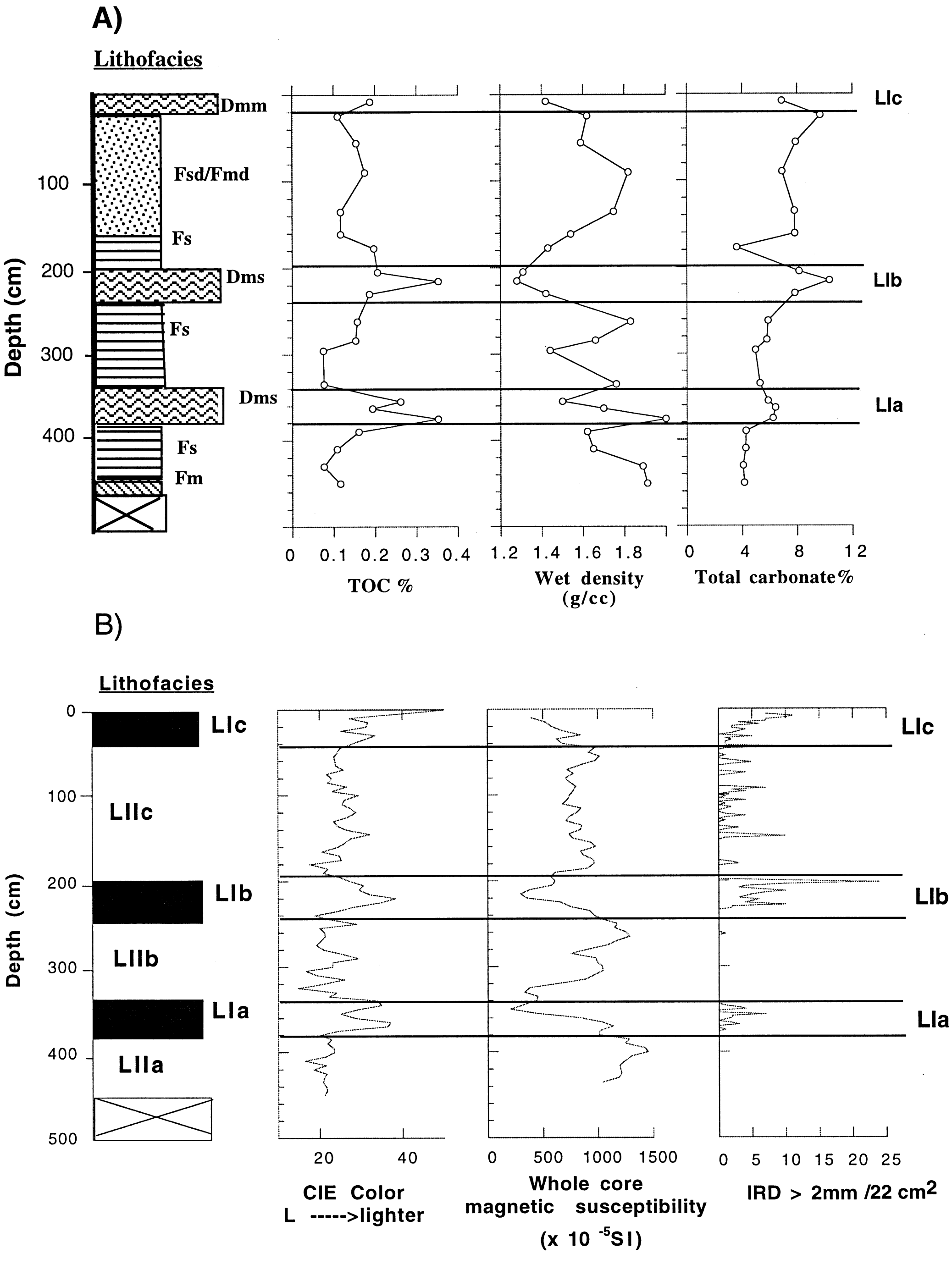

Fig. 5. (A) The facies to the left are based on interpretation of the X-radiography (*Dmm* = massive matrix-supported diamicton; *Fm* = fine-grained massive muds; *Fs* = fine-grained stratified sediments, the *d* refers to numerous drop stones. Weight% of TOC, wet vol. density, and %total carbonate. (B) Downcore variations in color (*L* has a range from 0 to 300, black to white), whole-core magnetic susceptibility ($\times 10^{-5}$ SI), clasts >2 mm/22 cm^2, and the lithofacies.

5.2. Sediment composition and provenance

The broad East Greenland shelf north of 007 (Fig. 1B) consists of Tertiary basalts, with an aggrading wedge of mid-Tertiary and younger sediments seaward of the mid-shelf (Larsen, 1983; Stein, 1996). Tertiary basalts form the outer coast between Kangerlussuaq Fjord and fjords to the north; they outcrop above Precambrian shield rocks (Brooks and Nielsen, 1982; Brooks, 1990). A variety of sedimentary rocks outcrop along the coast from Scoresby Sund northward.

The lithofacies log for the core (using the techniques of Eyles et al., 1983) was based on examination of the video X-radiography and description of the split core (Fig. 5A); other attributes that we used to define downcore changes included color and magnetic susceptibility (MS) (Fig. 5B). No. 007 contains two main lithofacies (I and II), namely diamictons (D) and fine-grained muds (F), respectively. Lithofacies I is classified as a stratified matrix-supported diamicton (Dms), comprised internally of interstratified matrix-supported diamicton (Dmm) and massive mud with dropstones (Fmd). Lithofacies II is a dark gray unit (5Y 3/1, 5Y 6/2) that is finer grained than LI and contains few if any clasts >2 mm. Lithofacies II is massive mud (Fm) at the base of the core, changing to stratified mud (Fs) upwards from the base of the core below LIa, and changing to stratified mud with dropstones (Fsd) above LIb. There is not a simple dichotomy in characteristics between Lithofacies I and II, although as shown in Fig. 5 there are some obvious differences in selected variables. For example, Lithofacies I is distinguished from LII by lower magnetic susceptibility (MS) and lighter color (2.5Y 6/2) (Fig. 5B). Lithofacies boundaries vary by a few centimeters depending on which criterion is used and are also, in detail, probably affected by changes in core length associated with transportation, drying, etc. Based on color and MS, LI occurs from 0 to 40 cm (LIc), 189 to 237 cm (LIb), and from 321 to 375 cm (LIa). Lithofacies Ia and Ib are correlated to distinct, narrow, parallel reflections on the Huntec profile across the site (Fig. 3). The boundaries between the two lithofacies are sharp but gradational.

As shown in Fig. 5A, the total carbonate content of the sediment increases gradually from bottom to top in the core, with peaks associated with the occurrence of LI. This pattern is mirrored in the percentage of carbonate clasts in the coarse fraction (G. Bond, pers. commun., 1996). Dolomite percentages are low and unvarying throughout the 4.5 m of sediment. Dowdeswell et al. (1995) show that the sediment thickness from Hudson Strait during H-1 and H-2 dramatically decreased across the North Atlantic; there is no a priori reason to suspect that the carbonate content in 007 is directly associated with IRD from Hudson Strait. Although a small fraction may represent biogenic carbonate, the majority probably represents glacial erosion of either Paleozoic limestones in NE Greenland, or possibly the erosion of mid-Tertiary and younger sedimentary rocks from the outer East Greenland shelf.

The number of clasts >2 mm are relatively low below 150 cm, except for the two discrete IRD peaks which obviously correlate with both the change in color and whole-core magnetic susceptibility (Fig. 5B). Above 150 cm in the core, the number of clasts >2 mm increases an LIIc is much coarser than the two underlying intervals of LII. The amount of basaltic glass in the >63 μm fraction reaches values of ~45% in unit Ib, whereas in LII values vary between 15 and 35% (G. Bond, pers. commun., 1996). The preliminary results from the >250 μm fraction (Fig. 6) show relatively little change in basaltic grains/g >250 μm.

Grain-size analyses of the <2 mm fraction indicates that sediments are sandy silts with modal peaks in the coarse to medium silt-size (Fig. 7). Sand-size material averages 40 ± 17% of the matrix with the largest fraction in the 63–125 μm size range. Surprisingly, there are no clear distinctions in grain-size spectra between LI and LII (Fig. 7). Values of TOC% show distinct peaks during LIa and LIb, and a less obvious rise in LIc. Wet sediment densities reveal no distinct differences between the lithofacies. The *S* rock magnetic parameter (Thompson and Oldfield, 1986) suggests a tendency for LI to contain slightly more hematite (lower values of *S*) than LII (not shown).

The estimated boundary dates indicate that the three intervals of LI have age ranges of: LIc = 14.3 to 15.5, LIb = 20.1 to 21.9, and LIa = 24.7 to 25.9 ka (Table 1; Fig. 4). The age estimates for LIc and LIb are thus slightly older than AMS radiocarbon dates from H-1 and H-2 events off Hudson Strait, associated with iceberg and sediment discharge from

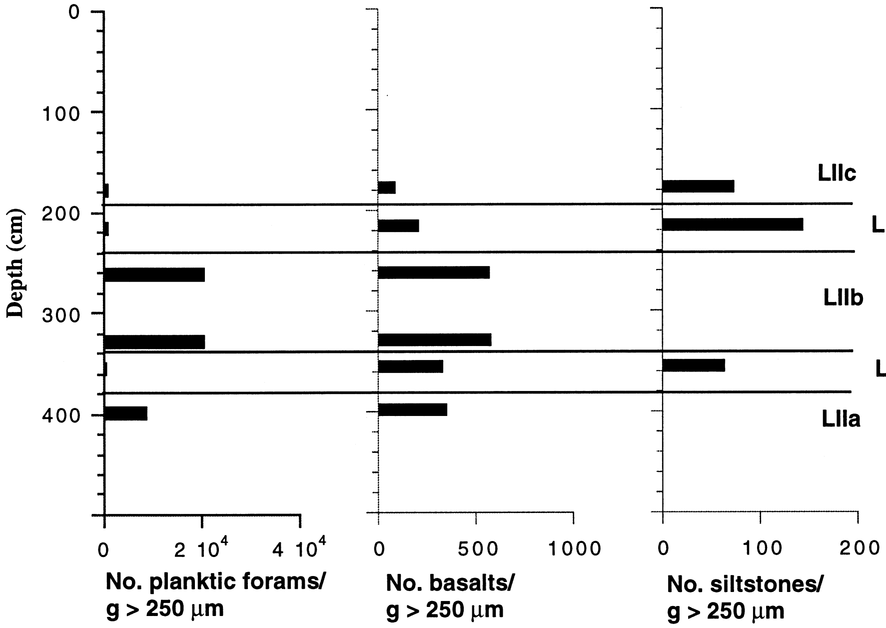

Fig. 6. Results of counts of ≥300 individuals ≥250 µm expressed as numbers per gram sediment ≥250 µm/g for six samples in and around Lithofacies Ia and Ib.

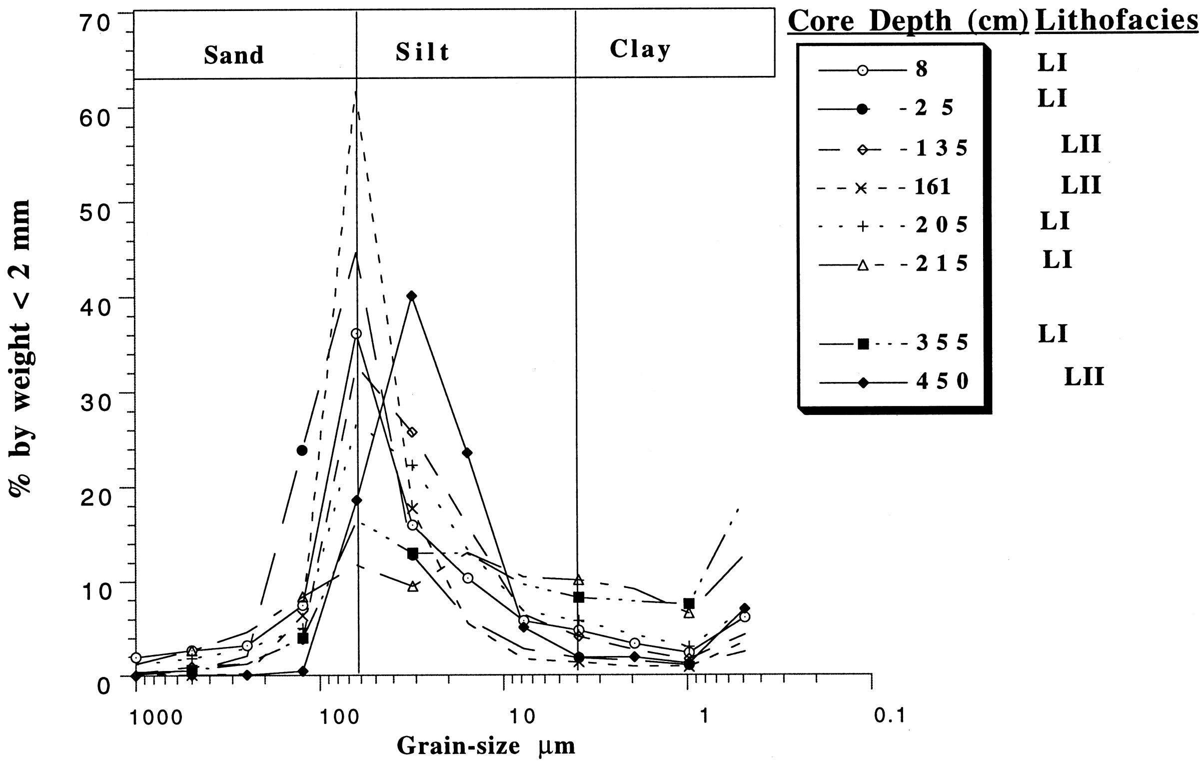

Fig. 7. Grain-size spectra (<2 mm) for selected levels in HU93030-007 from both Lithofacies I and II.

the Laurentide Ice Sheet (Andrews et al., 1994a; Jennings et al., 1996), and with IRD events in the North Atlantic (Bond et al., 1993; Bond and Lotti, 1995) (Table 1). However, in our age model, LIa is younger than previous estimates for H-3 (Fig. 4). All three units span an interval of $\geq$1 ka (Table 1). Regionally variable ocean reservoir values might be the cause of some discrepancies in age estimates, but this possibility is difficult to evaluate given our present knowledge.

5.3. Foraminiferal and isotope results >125 µm

Planktic foraminiferal concentrations average 1300/ml but diminish in abundance to a few hundred/ml during LIa (Fig. 8). A peak of ~8000/ml occurs immediately below LIb and another peak occurs at the boundary of Ic and within this unit. Therefore, the abundance of planktic foraminifera indicates a difference between the environment off East Greenland during Heinrich-like events and those in the classic areas of the North Atlantic (Heinrich, 1988; Bond et al., 1993; Bond and Lotti, 1995), where Heinrich intervals are frequently totally barren of foraminifera. The percentages of the polar, near-surface foraminifera, *N. pachyderma* sinistral, are mostly >95% suggesting a prevailing water temperature <5°C (Fig. 8). There is a tendency for the percentage of polar species to be lower in LII, especially in LIIb.

The planktic oxygen $\delta^{18}O$ isotope record increases from ≤4‰ at the base of the core to ~4.5‰ about 16 ka (Figs. 8 and 9). Changes in the $\delta^{18}O$ of the near-surface planktic foraminifera within LI are not dramatic. In the Nordic seas many records indicate the presence of a significant meltwater event 14–15 ka (Koc and Jansen, 1994; Hald and Andrews, 1995; Sarnthein et al., 1995; Sarnthein and Altenbach, 1995; Stein et al., 1996), but this event is not shown in our core, possibly because our record is truncated (Fig. 4). The benthic $\delta^{18}O$ record, however, shows somewhat lighter values during deposition of LIa and LIb (Fig. 8).

The difference (benthic $\delta^{18}O$ - planktic $\delta^{18}O$, $n = 25$) is a measure of change between the near-surface water conditions and those at ~1.8 km depth. The resulting plot suggests that during deposition of LI, the difference between benthic and planktic values decreases relative to the time when LII was the dominant sediment (Fig. 8). Median values for the differences are 0.73 and 1.09, respectively, for LI

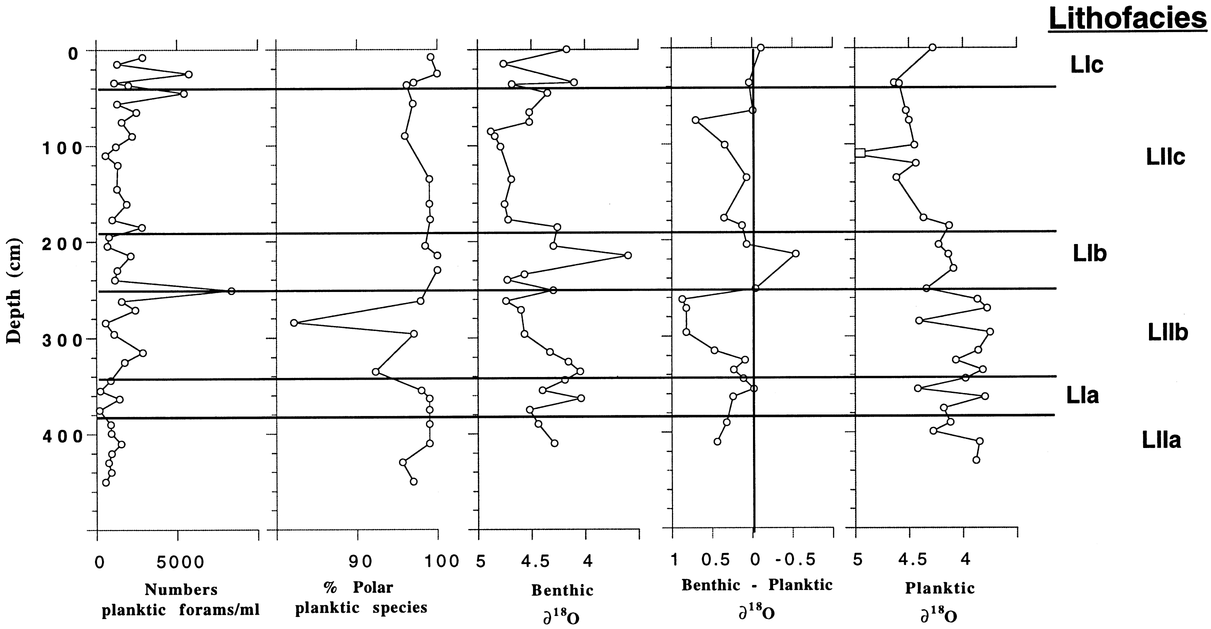

Fig. 8. Foraminifera data HU93030-007 (left to right): numbers of planktic foraminifera/ml; %polar planktic foraminifera; $\delta^{18}O$ of benthic species (see text); difference ($\delta^{18}O$ benthic - $\delta^{18}O$ planktic); $\delta^{18}O$ of planktic foraminifera.

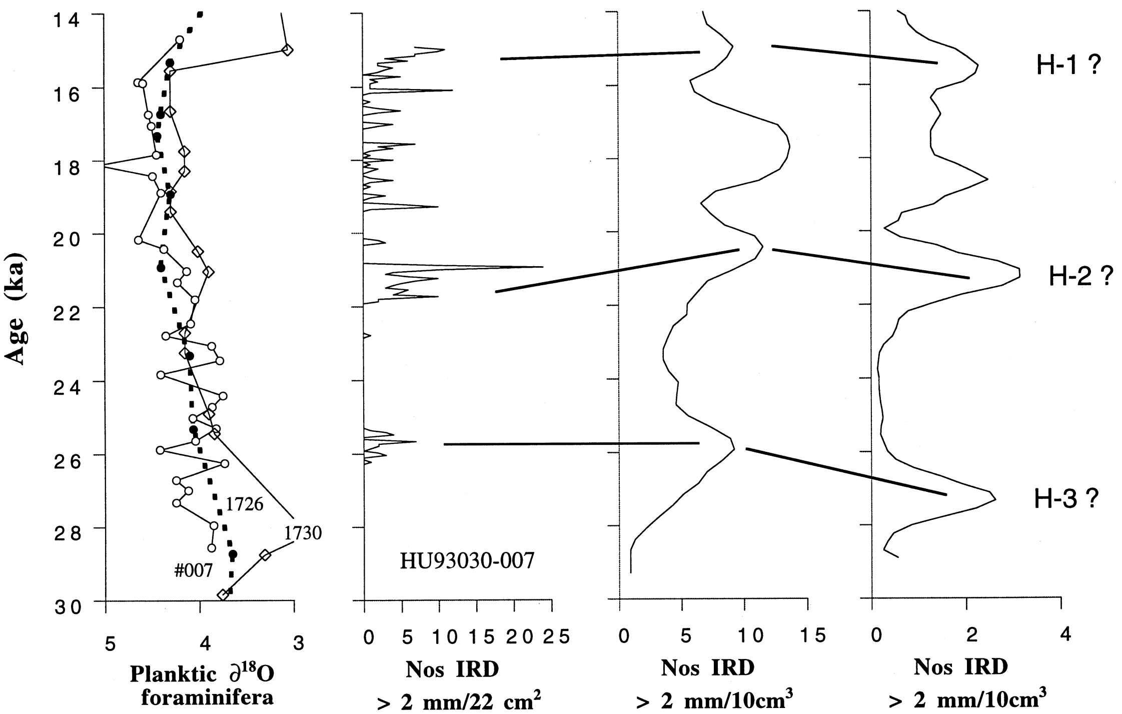

Fig. 9. Comparison of data from HU93030-007 and two cores from north of Denmark Strait (Stein et al., 1996) (Fig. 1A) plotted against age. (Left): the three $\delta^{18}O$ records (circles are core 007, dashed line is 1726, diamonds are 1730; the IRD counts for PS1726 and PS1730 (Stein et al., 1996) are in units of Nos. per 10 cm^3.

and LII, and the two data sets are statistically distinct at the $p = 0.01$ level.

We observed no major changes in benthic foraminiferal assemblages in the >250 μm fraction to parallel the alternation in lithofacies. Inspection of six samples for the >250 μm fraction, which were selected to be representative of Lithofacies I and II, indicates that the main difference between LI and LII is that LI contains tan siltstone clasts (Fig. 6). These sedimentary clasts impart the distinctive lighter color to LI; LII contains few or none of these sedimentary clasts except within LIIc. In addition, LI units have large numbers of partly lithified, immature sandstones rich in basaltic grains (not shown). They represent erosion and transport of till, or glacial marine sediments. The degree of consolidation suggests a Quaternary age.

5.4. 'Upstream' comparisons

North of Denmark Strait, Stein et al. (1996) examined the IRD and stable isotopes in two slope cores, PS1726 (1174 m wd, 70º0.7′N, 18º38.9′W) and PS1730 (1617 m wd, 70º07.2′N, 17º42.1′W) (Fig. 1A). The LGM ice margin is placed at the mouth of Scoresby Sund (Dowdeswell et al., 1994). Core chronology is constrained by the occurrence of the Vedde ash in both cores, and four and seven AMS radiocarbon dates, respectively. The data fit linear age models ($r^2 = 0.95$); these have been used to construct core chronologies (Fig. 9). The results indicate that sediment accumulation rates (SARs) are much slower for these two sites than 007 (~4 and 7 cm/ka, respectively).

Graphs of IRD from Stein et al. (1996) and IRD values derived by using the scanning program 'FlexiTrace™'. The $\delta^{18}O$ records from the three cores, graphed against a ^{14}C time-scale (Fig. 9), are very similar, especially between 26 and 15 ka. In PS1730 there is an abrupt meltwater event close to 15 ka and 28 ka. Because of the slow SAR there is not a great deal of resolution in PS1726. The IRD record from PS1726 (at the shallower depth) shows continuous IRD inputs with three broad peaks at

~26, 20, and 17 ka. PS1730 shows a much more on/off record with four IRD peaks; there is considerable similarity in the IRD signals between PS1730 and 007 (Fig. 8). All three of these East Greenland sites show an IRD event around 27–26 ka, a second one ~21–20 ka, and then a lengthy interval of IRD delivery <19 and >10 ka (Fig. 9). Given the errors in the linear SAR regression we cannot reject the hypothesis that the IRD events are coeval along the margin of East Greenland. Stein et al. (1996) correlated two of the peaks in PS1730 with events H-3 and H-2.

5.5. Comparison HU87033-009 and HU93030-007

A comparison between HU93030-007 from East Greenland and HU87033-009 (009) (62°30.99′N, 59°26.82′W; 1437 m wd; Table 1) from the slope north of Hudson Strait (Fig. 1A) is useful because both cores occupy similar relative positions with respect to: (a) south-flowing 'polar' shelf waters; (b) location immediately south of major sills (Denmark and Davis straits); (c) on slopes below areas where continental ice may have reached the shelf break; and (d) in a position where sediment could have transported parallel to the slope by deep-water currents (McCave et al., 1995). Heinrich events are represented in 009 by detrital carbonate-rich intervals (DC-events; Andrews and Tedesco, 1992; Andrews et al., 1994b) that are coeval with IRD events farther south in the North Atlantic (Bond et al., 1992). Our analysis of 009 (Jennings et al., 1996) concluded that shelf-dwelling benthic foraminifera were transported to the slope by glacial ice grounded on the shelf, especially during H-0 (Younger Dryas time) (Andrews et al., 1995). By contrast, the relative absence of such shelf benthic species in 007 supports an ice rafting origin for Lithofacies I over a debris flow origin.

In core 009 between 33 and 14 ka, the rate of sediment accumulation is 39 cm/ka (Fig. 4; Table 1). In Fig. 10 we show the $\delta^{18}O$ records of planktic foraminifera *N. pachyderma* sinistral. For both 007 and 009 (Andrews et al., 1994a; Cooper, 1995). The two records are very similar, indicating similar temperature/salinity conditions near the margins of both the NE Laurentide and East Greenland ice sheets (see also Fig. 9). Because of winnowing at the top of 007 we do not capture the dramatic decrease in

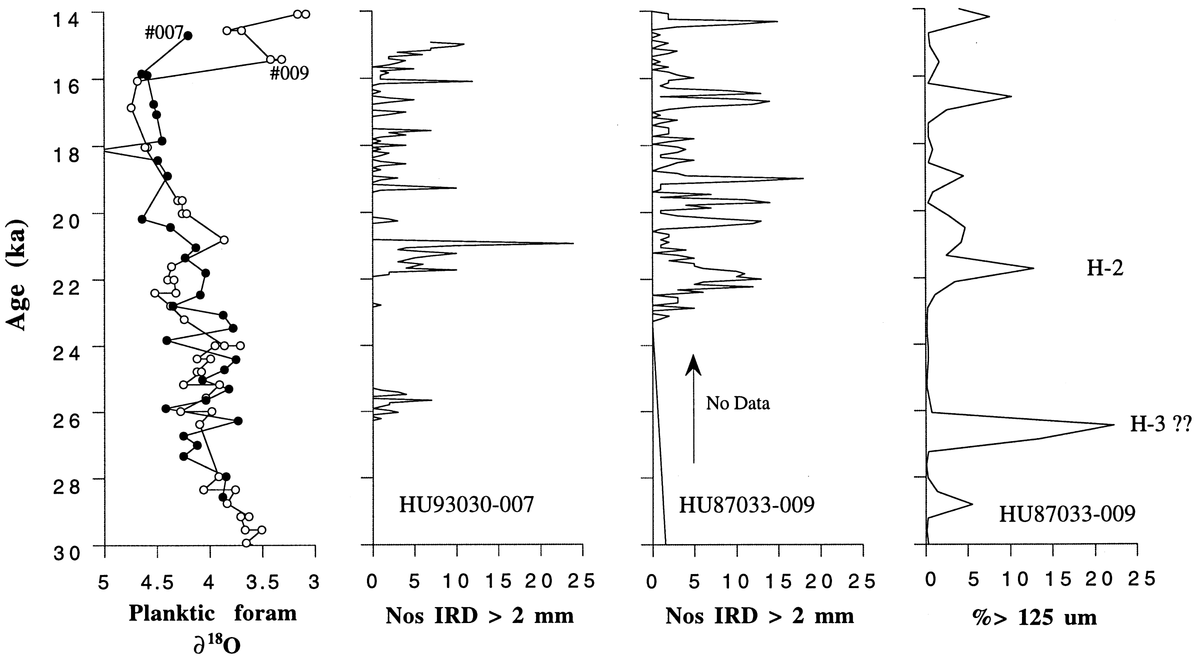

Fig. 10. Comparison of the near-surface planktic foraminiferal $\delta^{18}O$ records from HU87033-009 (Fig. 1A) and HU93030-007 plotted against interpolated radiocarbon time-scale, and compared against the IRD counts, and (far right) the >125 μm fraction in HU87033-009.

$\delta^{18}O$ associated with the 14–15 ka meltwater event (Koc and Jansen, 1994), but this event is evident in 009 and is also seen in PS1730 (Fig. 9). Neither 009 nor 007 shows any dramatic influence of meltwater during H-2 or H-3.

The IRD records from the two cores are based on the number of clasts >2 mm, but unfortunately the X-radiographs from 009 are of poor quality between 736 and 950 cm (Fig. 10). However, we show the >125–2000 μm fraction as a surrogate for IRD. The concentration of >2 mm IRD is similar in both cores (i.e. mean values of 2.1 ± 3.5 and 3.5 ± 4.1 clasts for 007 and 009 over the interval 14–23 ka). Although there is no distinct carbonate interval in 009 at the time of H-3 (Andrews and Tedesco, 1992; Andrews et al., 1998), there is a distinct peak in the >125 μm sand-size fraction.

6. Discussion

Sediment processes on glaciated continental margins, especially at the shelf/slope transition have been commented on by several authors (Piper, 1988; Piper et al., 1991; Yoon et al., 1991; Hesse, 1992; Andrews et al., 1994b; Hesse et al., 1996; Vorren and Laberg, 1997) (e.g. Fig. 2). It is worth noting, however, that there are no present-day analogs for these scenarios in the Northern Hemisphere. In a general sense, shelf/slope processes in these situations involve turbidity currents and debris flows, leading to development of major fans (Vorren et al., 1988; Vorren and Laberg, 1997) and/or large channel systems such as the North Atlantic Mid Ocean Channel (NAMOC) (Hesse, 1992; Hesse et al., 1996). These processes result in shelf erosion or deposition of till on the shelf, sediment failures on and from the slope, and sediment deposition in adjacent deep-sea basins from these and other meltwater-related processes (Fig. 2).

In 009, and other cores from the NW Labrador Sea, sediments coeval with H-events in the North Atlantic are sedimentologically much more complex than a simple IRD depositional model would imply (e.g. Hillaire-Marcel et al., 1994; Stoner et al., 1996). Depending on their location, Heinrich events are frequently fine-grained, laminated muds with an irregular IRD influx (Kirby, 1996; Wang and Hesse, 1996), and are associated with turbidite deposition from an ice margin assumed to be grounded at the shelf-edge (e.g. Fig. 2).

In 007 on the East Greenland slope, Lithofacies I could represent: (i) sediment gravity flows supplied by an ice margin at the shelf break; (ii) deposition from icebergs originating from ice margins to the north of Denmark Strait; and (iii) far-travelled icebergs originating from Hudson Strait, other sectors of the Laurentide Ice Sheet, or from ice sheets on the Eurasian shelf. In 007, IRD intervals average 47 cm in thickness and contain clasts up to 5 cm. The coarse-grained nature, large individual clasts, distinct color difference, and rarity of shelf benthic species leads to an interpretation that Lithofacies I represents hemipelagic sedimentation coupled with ice rafting. Potential sources for sand- and siltstones include the outer shelf, the Kangerlussuaq Fjord region, Scorsby Sund, and Svalbard (e.g. Hebbeln et al., 1994). During deposition of LIa and Lib a simple transfer function (fig. 10 in Andrews et al., 1997) forecasts ice advances across the shelf on 100 km or so.

Radiocarbon dates on sediments from Kangerlugssuaq Trough also assist in constraining the processes associated with deposition at 007 (Fig. 2). We have obtained a corrected date on an individual foraminifer at the base of JM96-1216, located close to K18B (Fig. 1B), of $14,420 \pm 135$ (AA-23222). We have also dated the base of a 3 m gravity core on the middle East Greenland shelf (PO175/1/5, Fig. 1B) at $14,300 \pm 190$ (Andrews et al., 1996). These dates from Kangerlugssuaq Trough are similar to that obtained from the top of 007 (about 14,500), which suggests either a very rapid retreat from the shelf break to the mid-shelf, or that the ice was not at the shelf break during the LGM (Fig. 1B, Fig. 2).

Cores from Kangerlugssuaq Trough (Fig. 1B) appear not to contain light brown sandstone clasts (Fig. 6), suggesting that there is no local source for this material and that an ice margin at the shelf edge was not responsible for deposition of these layers (Fig. 2). They may represent, therefore, more regional iceberg rafting events. Thus the alternate hypothesis (Stein, 1996) that these LI sediments are the result of debris flows from an ice margin on the shelf break, is not considered the most probable scenario, although we are still investigating evidence that will delimit the LGM ice margin on this portion of the East Greenland shelf.

7. Conclusions

Cores 007 and 009 (Fig. 1A, Fig. 10) record a series of distinct depositional events marked by changes in sediment provenance and in IRD concentrations. In both cores, magnetic susceptibility decreases during the IRD events. Dowdeswell et al. (1995) mapped the thickness of H-1 and H-2 and found that both layers are thickest in the northwest Labrador Sea and thin to the south and east, with a thickness <3 cm in Denmark Strait. It is improbable that the IRD intervals in 007 and PS1730 (Fig. 1A, Fig. 9) are associated with calving from the eastern margin of the Laurentide Ice Sheet. On the other hand, Stein et al.'s (1996) data from north of Denmark Strait are characterized by higher magnetic susceptibility during the IRD intervals, whereas 007 has low MS, and the SAR is a factor of 3 to 4 slower north of the strait. However, the actual magnetic susceptibility values in the cores north of Denmark Strait (Stein et al., 1996) are considerably lower that we report from 007 (Fig. 5B). These differences suggests that the sediment supply cannot be ascribed to a simple north$\rightarrow$south iceberg transportation route. It is interesting that on the Svalbard continental slope, Hebbeln et al. (1994) documented significant increases in sedimentary rock fragments and TOC% at times coeval with H-1 and H-2, but there is no equivalent change in their data during H-3 time. Thus although Svalbard could be a source for the tan siltstones in 007 (Fig. 6) it is noteworthy that in this East Greenland continental slope record these sedimentary rocks occur in Lithofacies Ia = H-3.

In the North Atlantic, H-events are defined by an increase in lithics, a decrease in foraminiferal abundance, and a shift in foraminiferal assemblages to a higher percentage of *N. pachyderma* sinistral (Heinrich, 1988; Bond et al., 1992). Several of these features correspond to characteristics of Lithofacies I, although there is no marked drop in total planktic foraminiferal abundance in the >125 μm fraction (Fig. 8).

The timing of the three IRD intervals in 007 and H-events in the North Atlantic (Bond and Lotti, 1995), warrants further comment. Are the ages for Lithofacies Ia, Ib and Ic such that a correlation with H-3, H-2 and H-1 is acceptable, or do they suggest that LIb and LIc lead H-2 and H-1 whereas Ia lags H-3? With the 'literature explosion' on Heinrich events since 1992 there has been too little critical dating of event boundaries for us to judge what the 'true' boundary dates are for H-1, H-2, and H-3.

Since the recognition of Heinrich events (Heinrich, 1988; Broecker et al., 1992) the debate has continued to grow concerning the origin of the events and the climatic implications that follow. If Heinrich events are produced by periodic binge and purge cycles of the Laurentide Ice Sheet (MacAyeal, 1993; Marshall and Clarke, 1998), then a glaciologic explanation is appropriate. If, on the other hand, they are produced by massive discharges of icebergs from the Fennoscandinavian and Greenland ice sheets, as well as the Laurentide Ice Sheet, then a more complex trigger mechanism(s) is needed. The presence of thick ice-rafted intervals both north and south of western Denmark Strait, possibly coeval with H-1, H-2, and H-3(?), is another piece of evidence indicating that H-events have a broader geographic distribution than can be expected from iceberg rafting from the LIS alone. What is presently unexplained is how a 'global' climate signal can so dramatically influence a variety of ice margins so as to produce a significant change in the flux of icebergs. McIntyre and Molfino (1996) have presented evidence that links H-events with sea-level fluctuations in the Equatorial North Atlantic, and it might be appropriate to reconsider the role of abrupt changes in relative sea level on the stability of ice sheet margins (cf. Thomas, 1977; Denton et al., 1986; Andrews, 1991).

Acknowledgements

Research has been supported by the National Science Foundation (Office of Polar Programs) and the Office of Naval Research, Grant OPP-9224254, and NOAA Consortium grant NA47GP0188. Ship time on *CSS Hudson* was supported by the Canadian Geological Survey of Canada and the Bedford Institute of Oceanography as part of the CANAM-PONAM project. We thank Dr. G. Bond for undertaking some counts for us and commenting on an early draft, and to D.C. Barber for his comments. Professor Jan Mangerud contributed significantly to this final presentation. Contribution no. SFB 343 of the Special Research Project of the German Research Council, Sonderforschungsbereich 313, at Kiel University. We thank the reviewers of this paper, Drs. Ruediger Stein and David Piper, for their critical reading and helpful comments.

References

Aagard, K., Fahrbach, E., Meincke, J., Swift, J.H., 1991. Saline outflow from the Arctic Ocean: Its contribution to the deep waters of the Greenland, Norwegian and Icelandic Seas. J. Geophys. Res. 96C, 20433–20441.

Alley, R.B., MacAyeal, D.R., 1994. Ice-rafted debris associated with binge-purge oscillations of the Laurentide Ice Sheet. Paleoceanography 9, 503–511.

Andrews, J.T., 1990. Fiord to deep-sea sediment transfers along the northeastern Canadian continental margin: Models and data. Geogr. Phys. Quat. 44, 55–70.

Andrews, J.T., 1991. Association of ice sheets and sea level with global warming: a geological perspective on aspects of global change. In: Bradley, R.S. (Ed.), Global Changes of the Past. UCAR/Office for Interdisciplinary Earth Studies, Boulder, CO, pp. 321–339.

Andrews, J.T., Freeman, W., 1996. The measurement of sediment color using the Colortron spectrophotometer. Arct. Alp. Res. 28, 524–528.

Andrews, J.T., Tedesco, K., 1992. Detrital carbonate-rich sediments, northwestern Labrador Sea: Implications for ice-sheet dynamics and iceberg rafting (Heinrich) events in the North Atlantic. Geology 20, 1087–1090.

Andrews, J.T., Erlenkeuser, H., Tedesco, K., Aksu, A., Jull, A.J.T., 1994a. Late Quaternary (Stage 2 and 3) meltwater and Heinrich events, NW Labrador Sea. Quat. Res. 41, 26–34.

Andrews, J.T., Tedesco, K., Briggs, W.M., Evans, L.W., 1994b. Sediments, sedimentation rates, and environments, SE Baffin Shelf and NW Labrador Sea 8 to 26 ka. Can. J. Earth Sci. 31, 90–103.

Andrews, J.T., Bond, G., Jennings, A.E., Kerwin, M., Kirby, M., MacLean, B., Manley, W., Miller, G.H., 1995. A Heinrich like-event, H-0 (DC-0): Source(s) for detrital carbonate in the North Atlantic during the Younger Dryas chronozone. Paleoceanography 10, 943–952.

Andrews, J.T., Jennings, A.E., Cooper, T., Williams, K.M., Mienert, J., 1996. Late Quaternary sedimentation along a fjord to shelf (trough) transect, East Greenland (ca. 68ºN). In: Andrews, J.T., Austin, W.E.N., Bergsten, H., Jennings, A.E. (Eds.), Late Quaternary Paleoceanography of North Atlantic Margins. Geol. Soc. London, Spec. Publ. 111, 153–166.

Andrews, J.T., Smith, L.M., Preston, R., Cooper, T., Jennings, A.E., 1997. Spatial and temporal patterns of iceberg rafting (IRD) along the East Greenland margin, ca. 68ºN, over the last 14 cal.ka. J. Quat. Sci. 12, 1–13.

Andrews, J.T., Kirby, M., Jennings, A.E., Barber, D.C., 1998. Late Quaternary stratigraphy, chronology, and depositional processes on the slope of SE Baffin Island, detrital carbonate and Heinrich events: Implications for onshore glacial history. Geogr. Phys. Quat., in press.

Asprey, K.W., Syvitski, J.P.M., Andrews, J.T., Dowdeswell, J.A., 1994. CANAM-PONAM Cruise HU93030: West Iceland to East Greenland. Geol. Surv. Can., Open-File Rep. 2824, 150 pp.

Bard, E., Arnold, M., Mangerud, J., Paterne, M., Labeyrie, L., Duprat, J., Melieres, M.-A., Sonstegaard, E., Duplessy, J.-C., 1994. The North Atlantic atmosphere–sea surface ^{14}C gradient during the Younger Dryas climatic event. Earth Planet. Sci. Lett. 126, 275–287.

Bennett, K.D., 1994. Confidence intervals for age estimates and deposition times in late-Quaternary sediment sequences. Holocene 4, 337–348.

Bond, G., 1994. Abrupt climate changes and ice rafting regimes in the North Atlantic-Progress Report. Abrupt Climate Change Program Notes, NOAA, Washington, D.C., pp. 1–2.

Bond, G.C., Lotti, R., 1995. Iceberg discharges into the North Atlantic on millennial time scales during the last glaciation. Science 267, 1005–1009.

Bond, G., Heinrich, H., Broecker, W.S., Labeyrie, L., McManus, J., Andrews, J.T., Huon, S., Jantschik, R., Clasen, S., Simet, C., Tedesco, K., Klas, M., Bonani, G., Ivy, S., 1992. Evidence for massive discharges of icebergs into the glacial Northern Atlantic. Nature 360, 245–249.

Bond, G., Broecker, W.S., Johnsen, S., McManus, J., Labeyrie, L., Jouzel, J., Bonani, G., 1993. Correlations between climate records from North Atlantic sediments and Greenland ice. Nature 365, 143–147.

Broecker, W.S., Denton, G.H., 1989. The role of ocean–atmosphere reorganizations in glacial cycles. Geochim. Cosmochim. Acta 53, 2465–2501.

Broecker, W.S., Bond, G., McManus, J., Klas, M., Clark, E., 1992. Origin of the Northern Atlantic's Heinrich events. Climatic Dyn. 6, 265–273.

Brooks, C.K. (Ed.), 1990. Kangerdlugssuaq Studies: Processes at a Rifted Continental Margin. Geological Institute, Univ. of Copenhagen, Copenhagen, 100 pp.

Brooks, C.K., Nielsen, T.F.D., 1982. The Phanerozoic development of the Kangerdlugssuaq area, East Greenland. Medd. Gronl., Geosci. 9, 1–30.

Cooper, T., 1995. Late Quaternary Ocean/Ice Sheet Interaction in Denmark Strait: Paleoceanographic and Paleoenvironmental Implications. Unpubl. MSc thesis, Univ. of Colorado, Boulder, 85 pp.

Denton, G.H., Hughes, T.J., 1981. The Last Great Ice Sheet. Wiley, New York, 484 pp.

Denton, G.H., Hughes, T.J., Karlen, W., 1986. Global ice-sheet system interlocked by sea level. Quat. Res. 26, 3–26.

Dowdeswell, J.A., Uenzelmann-Neben, G., Whittington, R.J., Marienfeld, P., 1994. The Late Quaternary sedimentary record in Scoresby Sund, East Greenland. Boreas 23, 294–310.

Dowdeswell, J.A., Maslin, M.A., Andrews, J.T., McCave, I.N., 1995. Iceberg production, debris rafting, and the extent and thickness of Heinrich layers (H-1, H-2) in North Atlantic sediments. Geology 23, 301–304.

Dreimanis, A., 1962. Quantitative gasometric determination of calcite and dolomite by using Chittick apparatus. J. Sediment. Petrol. 32, 520–529.

Eyles, C.H., Eyles, N., Miall, A.D., 1983. Lithofacies types and vertical profile models; an alternative approach to the description and environmental interpretation of glacial diamict and diamictite sequences. Sedimentology 30, 393–410.

Fronval, T., Jansen, E., Bloemendal, J., Johnsen, S., 1995. Oceanic evidence for coherent fluctuations in Fennoscandian and Laurentide Ice Sheets on millennium timescales. Nature 374, 443–445.

Funder, S., 1989. Quaternary geology of the ice — free areas and adjacent shelves of Greenland. In: Fulton, R.J. (Ed.), Quaternary Geology of Canada and Greenland. Geological Survey of Canada, Ottawa, ON, pp. 743–792.

Funder, S., Hansen, L., 1996. The Greenland ice-sheet — a model for its culmination and decay during and after the last glacial maximum. Bull. Geol. Soc. Denm. 42, 137–152.

Grobe, H., 1987. A simple method for the determination of ice-rafted debris in sediment cores. Polarforschung 57, 123–126.

Grousset, F.E., Labeyrie, L., Sinko, J.A., Cremer, M., Bond, G., Duprat, J., Cortijo, E., Huon, S., 1993. Patterns of ice-rafted detritus in the glacial North Atlantic (40–55ºN). Paleoceanography 8, 175–192.

Hald, M., Andrews, J.T., 1995. Response of the high-latitude Northern Hemisphere to orbital climate forcing: Evidence from the Nordic Seas: Comment and reply. Geology 23, 382–384.

Hebbeln, D., Dokken, T., Andersen, E.S., Hald, M., Elverhoi, A., 1994. Moisture supply for northern ice-sheet growth during the last glacial maximum. Nature 370, 357–360.

Heinrich, H., 1988. Origin and consequences of cyclic ice rafting in the Northeast Atlantic Ocean during the past 130,000 years. Quat. Res. 29, 143–152.

Hesse, R., 1992. Continental slope sedimentation adjacent to an ice margin, I. Seismic facies of Labrador slope. Geo-Mar. Lett. 12, 189–199.

Hesse, R., Klaucke, I., Ryan, W.B.F., Edwards, M.B., Piper, D.J.W., Group, N.S., 1996. Imaging Laurentide Ice Sheet drainage into the deep sea: Impact on sediments and bottom water. GSA Today (September): 3–9.

Hillaire-Marcel, C., de Vernal, A., Bilodeau, G., Wu, G., 1994. Isotope stratigraphy, sedimentation rates, deep circulation, and carbonate events in the Labrador Sea during the last ∼200 kyr. Can. J. Earth Sci. 31, 63–89.

Jennings, A.E., Tedesco, K.A., Andrews, J.T., Kirby, M.E., 1996. Shelf erosion and glacial ice proximity in the Labrador Sea during and after Heinrich events (H-3 or 4 to H-0) as shown by foraminifera. In: Andrews, J.T., Austin, W.E.N., Bergsten, H., Jennings, A.E. (Eds.), Late Quaternary Palaeoceanography of the North Atlantic Margins. Geol. Soc. London, Spec. Publ. 111, 29–49.

Johannessen, O.M., 1986. Brief overview of the physical oceanography. In: Hurdle, B.G. (Ed.), The Nordic Seas. Springer, New York, pp. 103–128.

Keigwin, L.D., Boyle, E.A., 1989. Late Quaternary Paleochemistry of high-latitude surface waters. Palaeogeogr., Palaeoclimatol., Palaeoecol. 73, 85–106.

Kellogg, T.B., 1984. Late-glacial/Holocene high-frequency climatic changes in deep-sea cores from the Denmark Strait. In: Mørner, N.A., Karlen, W. (Eds.), Climatic Changes on a Yearly to Millennial Basis. Reidel, Dordrecht, pp. 123–133.

King, J.W., Channell, J.E.T., 1991. Sedimentary magnetism, environmental magnetism, and magnetostratigraphy. Rev. Geophys., 24 Suppl., 358–370.

Kirby, M., 1996. Mid to Late Wisconsin Ice Sheet/Ocean Interactions in the Northwest Labrador Sea: Sedimentology, Provenance, Process, and Chronology. Unpubl. MSc thesis, Univ. of Colorado, Boulder, 194 pp.

Koc, N., Jansen, E., 1994. Response of the high-latitude Northern Hemisphere to orbital climate forcing: Evidence from the Nordic Seas. Geology 22, 523–526.

Lackschewitz, K.S., Baumann, K.H., Gehrke, B., Wallrabe-Adams, H.J., Thiede, J., Bonani, G., Endler, R., Erlenkeuser, H., Heinemeier, J., 1998. Late Quaternary northern ice sheet fluctuations: Evidence from short-term variations in the sediment composition of Reykjanes Ridge sediment cores. Quat. Res., submitted.

Larsen, B., 1983. Geology of the Greenland–Iceland Ridge in the Denmark Strait. In: Bott, M.H.P., Saxov, S., Talwani, M., Thiede, J. (Eds.), Structure and Development of the Greenland–Scotland Ridge. Plenum, London, pp. 425–444.

MacAyeal, D.R., 1993. Binge/purge oscillations of the Laurentide Ice Sheet as a cause of North Atlantic's Heinrich events. Paleoceanography 8, 775–784.

Malmberg, S.-A., 1985. The water masses between Iceland and Greenland. J. Mar. Res. Inst. 9, 127–140.

Manley, W.F., Jennings, A.E., 1996. Radiocarbon date list VIII: Eastern Canadian Arctic, Labrador, Northern Quebec, East Greenland Shelf, Iceland Shelf, and Antarctica. INSTAAR, Univ. of Colorado, Boulder, 163 pp.

Marshall, S.J., Clarke, G.K.C., 1998. A continuum mixture model of an ice stream thermomechanics in the Laurentide Ice Sheet, II. Application to the Hudson Strait Ice Steam. J. Geophys. Res., in press.

McCave, I.N., Tucholke, B.E., 1986. Deep current-controlled sedimentation in the western North Atlantic. In: Vogt, P.R., Tucholke, B.E. (Eds.), The Geology of North America: The Western North Atlantic Region. Geological Society of America, Boulder, CO, pp. 451–468.

McCave, I.N., Manighetti, B., Beveridge, N.A.S., 1995. Circulation in the glacial North Atlantic inferred from grain-size measurements. Nature 374, 149–152.

McIntyre, A., Molfino, B., 1996. Forcing of Atlantic Equatorial and subpolar millennial cycles by precession. Science 274, 1867–1870.

Mienert, J., Andrews, J.T., Milliman, J.D., 1992. The East Greenland continental margin (65ºN) since the last deglaciation:

Changes in sea floor properties and ocean circulation. Mar. Geol. 106, 217–238.
Nam, S.-I., Stein, R., Grobe, H., Hubberten, H., 1995. Late Quaternary glacial/interglacial changes in sediment composition at the East Greenland continental margin and their paleoceanographic implications. Mar. Geol. 122, 243–262.
Piper, D.J.W., 1988. Glaciomarine sedimentation on the continental shelf off eastern Canada. Geosci. Can. 15, 23–28.
Piper, D.J.W., Mudie, P.J., Fader, G.B., Josenhans, H.W., MacLean, B., Vilks, G., 1991. Quaternary Geology. In: Keen, M.J., Williams, G.L. (Eds.), Geology of the Continental Margin of Eastern Canada. Geological Society of America, Boulder, CO, pp. 475–607.
Rahman, A., 1995. Reworked nannofossils in the North Atlantic Ocean and subpolar basins: Implications for Heinrich events and ocean circulation. Geology 23, 487–490.
Robinson, S.G., Maslin, M.A., McCave, N., 1995. Magnetic susceptibility variations in Upper Pleistocene deep-sea sediments of the NE Atlantic: Implications for ice rafting and palaeocirculation at the last glacial maximum. Paleoceanography 10, 221–250.
Sarnthein, M., Altenbach, A.V., 1995. Late Quaternary changes in surface water and deep water masses of the Nordic Seas and north-eastern North Atlantic: a review. Geol. Rundsch. 84, 89–107.
Sarnthein, M., and fourteen others, 1995. Variations in Atlantic surface ocean paleoceanography, 50º–80ºN: A time-slice record of the last 30,000 years. Paleoceanography 10, 1063–1094.
Shackleton, N.J., 1973. Attainment of isotopic equilibrium between ocean water and the benthic foraminifera genus *Uvigerina*: Isotopic changes in the ocean during the last glacial. Colloq. Int. C.N.R.S. 219, 203–209.
Sommerhoff, V.G., 1981. Geomorphologische Prozesse in der Labrador- und Irmingersee. Ein Beitrag zur submarinen Geomorphologie einer subpolaren Meeresregion. Polarforschung 51, 175–191.
Sommerhoff, V.G., Larsen, B., Michier, G., 1979. Zur Frage der topographischen Steuerung der ozeanischen Polarfront vor Sudgronland. Polarforschung 48, 63–69.
Stata, 1996. Stata Release 5. Stata Press, College Station, TX, five volumes.
Stein, A., 1996. Seismic Stratigraphy and Seafloor Morphology of the Kangerlugssuaq Region, East Greenland: Evidence for Glaciations to the Continental Shelf Break During the Late Weichselian Age and Earlier. MSc thesis, Univ. of Colorado, Boulder, 293 pp.
Stein, R., Nam, S.-I., Grobe, H., Hubberten, H., 1996. Late Quaternary glacial history and short-term ice-rafted debris fluctuations along the East Greenland continental margin. In: Andrews, J.T., Austen, W.A., Bergsten, H., Jennings, A.E. (Eds.), Late Quaternary Paleoceanography of North Atlantic Margins. Geol. Soc. London, Spec. Publ. 111, 135–151.
Stoner, J.S., Channell, J.E.T., Hillaire-Marcel, C., 1996. The magnetic signature of rapidly deposited detrital layers from the deep Labrador Sea: Relationship to North Atlantic Heinrich layers. Paleoceanography 11, 309–326.
Swift, J.H., 1986. The Arctic waters. In: Hurdle, B.G. (Ed.), The Nordic Seas. Springer, New York, pp. 129–154.
Syvitski, J.P.M., 1991. Towards an understanding of sediment deposition on glaciated continental shelves. Cont. Shelf Res. 11, 897–937.
Thomas, R.H., 1977. Calving Bay dynamics and ice sheet retreat up the St. Lawrence Valley system. Geogr. Phys. Quat. 31, 347–356.
Thomas, R.H., Bentley, C.R., 1978. A model for Holocene retreat of the West Antarctic Ice Sheet. Quat. Res. 10, 150–170.
Thompson, R., Oldfield, F., 1986. Environmental Magnetism. Allen and Unwin, Winchester, MA, 227 pp.
Voelker, A.H.L., Sarnthein, M., Grootes, P., Erlenkeuser, Laj, C., Mazaud, A., Nadeau, M.J., Schleicher, M., 1997. Calibration of ^{14}C ages in deep-sea core PS2644 from the Iceland Sea to GISP2 ice-core calendar ages over the interval 25–50 kyr ago. Radiocarbon. Proc. Groningen ^{14}C Conf.
Vorren, T.O., Laberg, J.S., 1997. Trough mouth fans — Paleoclimate and ice-sheet monitors. Quat. Sci. Rev. 16, 865–886.
Vorren, T.O., Andreassen, K., Larsen, K.B., Lebesbye, E., 1988. Glacigenic sediments on a passive continental margin as exemplified by the Barents Sea. Mar. Geol. 85, 251–272.
Walkley, A., 1947. A critical examination of a rapid method for determining organic carbon in soils. Effects of variation in digestion conditions of inorganic soil constituents. Soil Sci. 63, 251–264.
Wang, D., Hesse, R., 1996. Continental slope sedimentation adjacent to an ice margin. II. Glaciomarine depositional facies on Labrador Slope and glacial cycles. Mar. Geol. 135, 65–96.
Williams, K.M., 1993. Ice sheet and ocean interactions, margin of the East Greenland Ice Sheet (14 ka to present): Diatom evidence. Paleoceanography 8, 69–83.
Williams, K.M., Andrews, J.T., Weiner, N.J., 1995. Late Quaternary paleoceanography of the mid- to outer continental shelf, East Greenland. Arct. Alp. Res. 27, 352–363.
Yoon, S.H., Chough, S.K., Thiede, J., Werner, F., 1991. Late Pleistocene sedimentation on the Norwegian continental slope between 67 degrees and 71 degrees N. Mar. Geol. 99, 187–207.